 

# Material Design and High-Pressure Synthesis of Novel *A*-Site-Ordered Perovskites $A$Mn$_3$Al$_4$O$_{12}$ ($A$ = Y, Yb, and Dy) with Square-Planar-Coordinated Mn$^{3+}$

**Takashi Saito,*[1] Takenori Tohyama,[1] Patrick M. Woodward,[2] and Yuichi Shimakawa[1]**

[1]Institute for Chemical Research, Kyoto University, Gokasho, Uji, Kyoto 611-0011

[2]Department of Chemistry, Ohio State University, 100 West 18th Avenue, Columbus, Ohio 43210, USA

Received November 29, 2010; E-mail: saito@scl.kyoto-u.ac.jp

Structural stability of *A*-site-ordered perovskites $A$Mn$_3$Al$_4$O$_{12}$ was evaluated by the global instability index calculated from the *SPuDS* program. Based on the results, we "designed" new compounds $A$Mn$_3$Al$_4$O$_{12}$ ($A$ = Y, Yb, and Dy), and these compounds were synthesized with a high-pressure technique. The obtained compounds were ionic crystals, $A^{3+}$Mn$^{3+}{}_3$Al$^{3+}{}_4$O$^{2-}{}_{12}$, with fourfold square-planar coordination for Mn$^{3+}$ at the originally twelvefold-coordinated $A$ site of the $AB$O$_3$ simple perovskite structure. Structural parameters obtained from the structure refinement well agreed with the "predicted" values. The synthesized compounds contained magnetic Mn$^{3+}$ ions with $S = 2$ spins at the $A'$ site, and the $A'$–$A'$ interaction resulted in antiferromagnetic ordering of the Mn$^{3+}$ spins at temperatures ranging from 29 to 40 K. The Yb$^{3+}$/Dy$^{3+}$ moments in (Yb/Dy)Mn$_3$Al$_4$O$_{12}$ were found to be paramagnetic even below the antiferromagnetic transition temperatures.

*A*-site-ordered perovskite oxides with chemical formula $AA'_3B_4O_{12}$ have a rich variety of physical and chemical properties, such as the large dielectric response of CaCu$_3$Ti$_4$O$_{12}$,[1] the giant magnetoresistance of (Ca/La/Bi)Cu$_3$Mn$_4$O$_{12}$,[2–4] and the intersite charge transfer seen in LaCu$_3$Fe$_4$O$_{12}$.[5] They have a transition-metal (TM) ion at the $A'$ site (3/4 of the $A$ site of a simple perovskite $AB$O$_3$), because the $B$O$_6$ octahedra in the $2a \times 2a \times 2a$ unit cell ($a$: unit cell of a simple cubic perovskite) are heavily tilted to form fourfold square-planar coordination at the $A'$ site, as illustrated in Figure 1. The partially filled d bands of the TM ions at the $A'$ site enable electronic and magnetic correlations between $A'$ and $A'$ sites and/or $A'$ and $B$ sites, in addition to the ordinary $B$–$B$ correlation, giving rise to novel properties beyond simple $AB$O$_3$ perovskites.

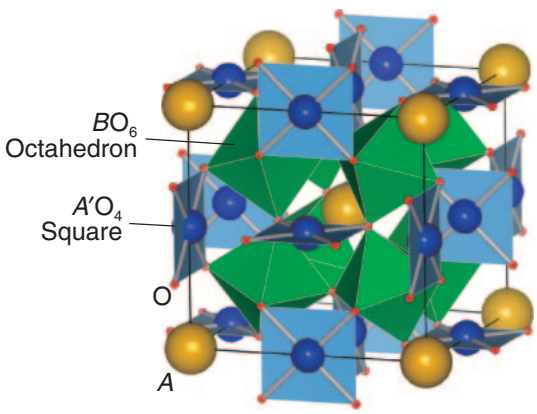


**Figure 1.** Crystal structure of *A*-site-ordered perovskite $AA'_3B_4O_{12}$. The *A*-site ions (yellow spheres) and $A'$-site ions (blue spheres) are ordered at a 1:3 ratio at the $A$ sites of the $AB$O$_3$ perovskite structure, and the $B$-site ions form $B$O$_6$ octahedra (green) in a cubic perovskite structure.

From the structural point of view, the flexibility for rotating and/or tilting the $B$O$_6$ octahedra in the $AA'_3B_4O_{12}$ perovskites is rather limited because of the need to maintain the square-planar coordination at the originally twelvefold-coordinated $A$ site in the simple perovskite. Therefore the sizes and valences of the constituent ions have to be properly fitted to stabilize the crystal structure. The number of the $AA'_3B_4O_{12}$ perovskites that have been made is rather small, and most of them are synthesized under high-pressure conditions (several gigapascals), suggesting that such a crystal structure type can often be stabilized under high pressure.

In this paper we focus on the synthesis of newly designed *A*-site-ordered perovskites with the formula $A^{3+}$Mn$^{3+}{}_3$Al$^{3+}{}_4$O$_{12}$. Such compounds with nonmagnetic $A^{3+}$ ions would enable us to study the magnetic properties of the Mn$^{3+}$ spins at the square-planar $A'$ sites, because Al$^{3+}$ ion is nonmagnetic. The number of $A$Mn$_3B_4$O$_{12}$ perovskites with Mn ions at the $A'$ sites is very small—$A$Mn$_7$O$_{12}$,[6] LaMn$_3B_4$O$_{12}$ ($B$ = Cr and Ti),[7] and YMn$_3$Al$_4$O$_{12}$[8]—and Mn$^{3+}$ ions with square-planar coordination are rare in oxides. The magnetic properties of $A^{3+}$Mn$^{3+}{}_3$Al$^{3+}{}_4$O$_{12}$ are therefore of interest, and the study of these compounds would provide information useful for the future development of functional *A*-site-ordered perovskites. We have previously reported the unusual $A'$-site magnetism seen in the *A*-site-ordered perovskites CaCu$_3$Ge$_4$O$_{12}$, CaCu$_3$Ti$_4$O$_{12}$, and CaCu$_3$Sn$_4$O$_{12}$, where the magnetic interaction of $A'$-site Cu$^{2+}$ spins changes from ferromagnetic to antiferromagnetic to ferromagnetic with increasing size of the $B$-site ion.[9] Differences in the behavior of Mn$^{3+}$ spins at the $A'$ site from that of Cu$^{2+}$ spins are of interest.

Published on the web July 2, 2011; doi:10.1246/bcsj.20100335

The rigidity of the $AA'_3B_4O_{12}$ structure, coupled with the time and cost associated with high-pressure synthetic routes place a premium on intelligent choice of target compositions. Therefore, we turned to the *SPuDS* software program[10,11] to guide our synthetic efforts. Previous studies have shown *SPuDS* to be effective in guiding high-pressure synthesis of perovskites.[12–15] Here we repost this design and synthesis of the *A*-site-ordered perovskites $A$Mn$_3$Al$_4$O$_{12}$ ($A$ = Y, Yb, and Dy) and discuss the magnetic properties of their $A'$-site $Mn^{3+}$ spins.

## Calculation and Experimental Methods

The structural stability of hypothetical perovskite compounds was evaluated using the *SPuDS* program, in which the stability of a perovskite structure with a given composition is specified by a global instability index (GII) equal to $\{[\Sigma_i\{V_i(\mathrm{OX}) - V_i(\mathrm{calc})\}^2]/N\}^{1/2}$, where $N$ is the number of atoms in the formula unit and $V_i$(OX) and $V_i$(calc) are the formal valence and the calculated bond valence sum (BVS) for the $i$-th ion, respectively. In the calculation, the $B$–O distance was fixed to a value to give $V_B(\mathrm{calc}) = V_B(\mathrm{OX})$, while the lattice parameters as well as the fractional coordinates of O were optimized so as to minimize the GII. Empirically, perovskite oxides with GII below 0.1 can often be synthesized. In the present calculation we focused on *A*-site-ordered perovskite oxides with $Im\bar{3}$ symmetry (Glazer tilt system[16] $a^+a^+a^+$) accommodating Mn ions at the $A'$ sites and Al ions at the *B* sites. We evaluated the structural stability of $A$Mn$_3$Al$_4$O$_{12}$ with lanthanoid ions and Y ions at the *A* site because these ions are often accommodated at the *A* site in the simple perovskite structure. The formal valences of all the cations were set to +3, and the formal valence of oxygen ion was set to −2.

The polycrystalline $A$Mn$_3$Al$_4$O$_{12}$ perovskite samples were prepared in a solid-state reaction under high pressure using a cubic anvil press.[8] Lanthanoid oxide raw materials were preheated at 1000 °C for 12 h before use. Stoichiometric amounts of $Al_2O_3$, $Mn_2O_3$, and $Y_2O_3$/$Dy_2O_3$/$Yb_2O_3$/$La_2O_3$ were well mixed, sealed in a gold capsule, held at 900 °C under 9 GPa for 1 h, and then cooled for 5 h to room temperature before the pressure was released. Formation of the *A*-site-order perovskite phase was checked by X-ray diffraction using Cu K$\alpha$ radiation. Synchrotron X-ray diffraction patterns of the polycrystalline $A$Mn$_3$Al$_4$O$_{12}$ samples were also collected on a Debye–Scherrer camera installed at beamline BL02B2 of SPring-8 in Japan, with a wavelength of 0.778256 Å for DyMn$_3$Al$_4$O$_{12}$ and YbMn$_3$Al$_4$O$_{12}$ and of 0.778084 Å for YMn$_3$Al$_4$O$_{12}$. Rietveld refinements of the diffraction data were done using the program *RIETAN-2000*.[17] Magnetic properties were measured using a SQUID magnetometer (Magnetic Property Measurement System, Quantum Design), and specific heat measurements were done by the thermal relaxation method (Physical Property Measurement System, Quantum Design).

## Results and Discussion

The GIIs obtained by *SPuDS* for the hypothetical $A$Mn$_3$Al$_4$O$_{12}$ perovskites ($A$ = lanthanoids, Y) are shown in Figure 2. The ionic radii $r_A$ for trivalent *A*-site ions shown here for comparison are those for ninefold coordination because those for twelvefold coordination are not available for some lanthanoids. GII first decreases as $r_A$ increases, reaches a minimum for Dy, and then increases. The calculated BVS of Mn at the $A'$ site gradually decreases with increasing $r_A$ but remains close to its formal valence, +3. The calculated BVS of the *A*-site ion, on the other hand, increases significantly and for La is over +4. The *SPuDS* results therefore suggest that synthesis of $A$Mn$_3$Al$_4$O$_{12}$ compositions with $A^{3+}$ ions having $r_A$ near 1.08 Å offer the highest probability of success. We thus decided that $A$Mn$_3$Al$_4$O$_{12}$ with $A$ =Y, Yb, and Dy would make the best target compositions for synthesis. We also tried to synthesize LaMn$_3$Al$_4$O$_{12}$ for comparison. The detailed results of the *SPuDS* calculations for $A$Mn$_3$Al$_4$O$_{12}$ with $A$ = Y, Yb, Dy, and La are listed in Table 1.

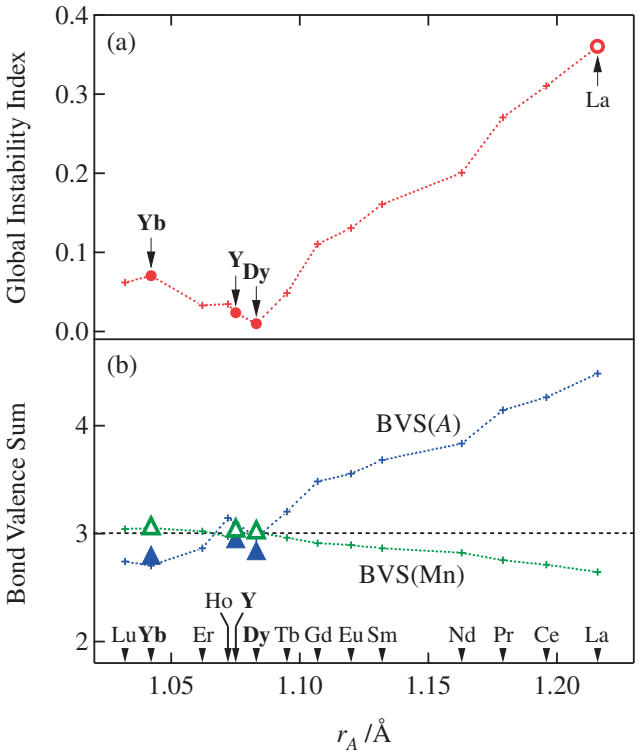


**Figure 2.** Global instability index (a) and bond valence sum (BVS) (b) for $A$Mn$_3$Al$_4$O$_{12}$ ($A = Y^{3+}$, trivalent lanthanoids) obtained from the *SPuDS* calculation. BVS values experimentally obtained from the structural refinement for the synthesized compounds are also shown (filled and open triangles represent *A* and Mn ions, respectively). Ionic radii of ninefold coordinated *A*-site ions are used for comparison.

Syntheses under ambient pressure were not successful, yielding mainly $Al_2O_3$, $AMn_2O_5$, and some other minor phases for $A$ = Y, Yb, and Dy, and $LaMnO_3$, $Al_2O_3$, and $(Mn,Al)_3O_4$ spinel for $A$ = La, instead. However, YMn$_3$Al$_4$O$_{12}$, YbMn$_3$Al$_4$O$_{12}$, and DyMn$_3$Al$_4$O$_{12}$ were obtained under high-pressure conditions. This implies that the *A*-site-ordered perovskites with $A$ = Y, Yb, and Dy become the most stable phases under high pressures, though they are not the most stable ones at ambient pressure. Since the $ABO_3$ perovskites have a close-packed structure of *A* and O ions, high pressure often helps to stabilize oxides with the perovskite-type structure. LaMn$_3$Al$_4$O$_{12}$, on the other hand, could not be synthesized even under 9 GPa, where LaMn$_3$Mn$_4$O$_{12}$, $LaAlO_3$, and $Al_2O_3$ were

**Table 1.** Results of *SPuDS* Calculation for $AMn_3Al_4O_{12}$ ($A$ = Yb, Y, Dy, and La)[a)]

| $A$ | Yb | Y | Dy | La |
|---|---|---|---|---|
| $r_A$ | 1.042 | 1.075 | 1.083 | 1.216 |
| GII | 0.070 | 0.023 | 0.0093 | 0.36 |
| Lattice parameter/Å | 7.1135 | 7.1223 | 7.1193 | 7.1710 |
| $y$(O) | 0.1840 | 0.1849 | 0.1846 | 0.1898 |
| $z$(O) | 0.3022 | 0.3017 | 0.3019 | 0.2985 |
| Bond length | | | | |
| $A$–O (×12)/Å | 2.5169 | 2.5199 | 2.5189 | 2.5367 |
| Mn–O (×4)/Å | 1.9216 | 1.9310 | 1.9277 | 1.9852 |
| Mn–O (×4)/Å | 2.6519 | 2.6520 | 2.6520 | 2.6524 |
| Mn–O (×4)/Å | 3.1105 | 3.1071 | 3.1083 | 3.0870 |
| Al–O (×6)/Å | 1.8765 | 1.8765 | 1.8765 | 1.8765 |
| Bond angle | | | | |
| Al–O–Al/degree | 142.79 | 143.21 | 143.06 | 145.64 |
| Bond valence sum | | | | |
| $A$ | 2.70 | 3.10 | 2.96 | 4.48 |
| Mn | 3.05 | 2.98 | 3.01 | 2.65 |
| Al | 3.00 | 3.00 | 3.00 | 3.00 |
| O | 1.99 | 2.00 | 2.00 | 2.03 |

a) The initial formal valences of all the cations were set to +3 in the calculation. The ionic radii $r_A$ for trivalent $A$-site ions in ninefold coordination are also listed.

obtained instead. These experimental results are consistent with the *SPuDS* calculation results that GIIs for $YMn_3Al_4O_{12}$, $YbMn_3Al_4O_{12}$, and $DyMn_3Al_4O_{12}$ are less than 0.1, while that for $LaMn_3Al_4O_{12}$ is more than 0.3. The bond valence sum calculated by *SPuDS* for La in $LaMn_3Al_4O_{12}$ was 4.48, which indicates that $La^{3+}$ is too large to fit into the 12-coordinate cavity in the $Mn_3Al_4O_{12}{}^{3-}$ network. The only way to reduce its BVS at the La site is to reduce the tilt angle, but that is unfavorable because it leads to underbonding at the Mn site.

The synchrotron X-ray powder diffraction patterns of $YMn_3Al_4O_{12}$, $YbMn_3Al_4O_{12}$, and $DyMn_3Al_4O_{12}$ are shown in Figure 3 along with the Rietveld fitting results. Although a small amount of impurities were detected in the refinements, the major peaks in each pattern were well reproduced with a cubic $Im\bar{3}$ $AA'_3B_4O_{12}$ perovskite structure model. In the initial refinements of each pattern, some disagreement in the diffraction intensities suggested cation substitutions. Incorporation of Mn ions into the $B$ site was thus included in the final refinements. The amount of cation substitution at the $B$ site by Mn was in the range 2.6–5.5%. Incorporating Al ions into the $A'$ site did not improve the refinement. We note here that the difference in the atomic form factors of $Mn^{3+}$ and $Al^{3+}$ with total numbers of electrons of 22 and 10, respectively, is large enough to distinguish these cations by X-ray. No anomalies were found in the oxygen occupancies. The structural parameters obtained from the refinements are listed in Table 2, and some selected bond lengths and angles are also listed in Table 3 along with the BVS obtained from the refined bond lengths. The obtained BVS values agree well with those estimated in the *SPuDS* calculations, and the results indicate a charge state of $A^{3+}Mn^{3+}{}_3Al^{3+}{}_4O^{2-}{}_{12}$ for all three cases. For each compound the four short Mn–O distances clearly show the square-planar

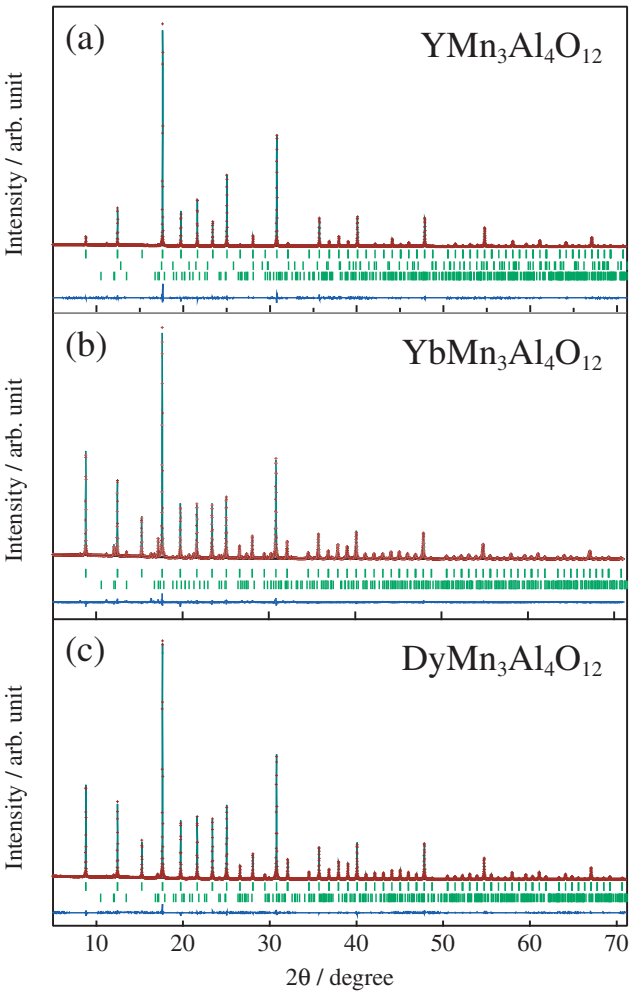


**Figure 3.** Synchrotron X-ray powder diffraction patterns and Rietveld fitting results for $AMn_3Al_4O_{12}$ ($A$ = Y, Yb, and Dy). The observed (+) and calculated (line) intensities and their difference (bottom line) are shown. The ticks indicate the allowed Bragg reflections. Small amounts of $Al_2O_3$ and $YAlO_3$ impurities for $YMn_3Al_4O_{14}$, $YbAlO_3$ impurities for $YbMn_3Al_4O_{14}$, and $DyAlO_3$ impurities for $DyMn_3Al_4O_{14}$ were included in the refinements.

**Table 2.** Refined Structural Parameters and $R$-Factors Obtained by Rietveld Analysis of Synchrotron X-ray Powder Diffraction Data for $AMn_3Al_4O_{12}$ ($A$ = Yb, Y, and Dy)

| Formula | $YbMn_3Al_4O_{12}$ | $YMn_3Al_4O_{12}$ | $DyMn_3Al_4O_{12}$ |
|---|---|---|---|
| Lattice parameter/Å | 7.17211(1) | 7.17962(1) | 7.18387(1) |
| $U_{iso}(A)$/Å$^2$ | 0.0044(1) | 0.0023(1) | 0.00308(6) |
| $U_{iso}$(Mn)/Å$^2$ | 0.0035(1) | 0.0041(5) | 0.00459(7) |
| $g(Mn)_{8c}$[a)]/% | 5.5(3) | 4.8(1) | 2.6(2) |
| $U_{iso}$(Al)/Å$^2$ | 0.0029(2) | 0.0027(1) | 0.0026(1) |
| $y$(O) | 0.1812(2) | 0.1811(2) | 0.1814(1) |
| $z$(O) | 0.3035(2) | 0.3033(1) | 0.3039(1) |
| $U_{iso}$(O)/Å$^2$ | 0.0084(4) | 0.0070(3) | 0.0073(3) |
| $R_{wp}$/% | 3.63 | 4.52 | 2.93 |
| $R_B$/% | 2.63 | 2.42 | 2.91 |

a) $g(Mn)_{8c}$ represents the occupancy of Mn at the 8$c$(Al) site (1/4, 1/4, 1/4).

**Table 3.** Selected Bond Lengths, Bond Angles, and BVS for $A$Mn$_3$Al$_4$O$_{12}$ ($A$ = Yb, Y, and Dy)

| Formula | $YbMn_3Al_4O_{12}$ | $YMn_3Al_4O_{12}$ | $DyMn_3Al_4O_{12}$ |
|---|---|---|---|
| Bond length | | | |
| $A$–O (×12)/Å | 2.535(1) | 2.537(1) | 2.5429(9) |
| Mn–O (×4)/Å | 1.917(1) | 1.9195(9) | 1.9190(8) |
| Mn–O (×4)/Å | 2.686(1) | 2.690(1) | 2.6872(9) |
| Mn–O (×4)/Å | 3.157(1) | 3.1598(9) | 3.1631(8) |
| Al–O (×6)/Å | 1.8989(4) | 1.9008(3) | 1.9022(3) |
| Bond angle | | | |
| Al–O–Al/degree | 141.56(7) | 141.58(5) | 141.53(5) |
| Bond valence sum | | | |
| $A$ | 2.71 | 2.92 | 2.77 |
| Mn | 3.04 | 3.01 | 3.02 |
| Al | 3.01 | 3.00 | 2.99 |
| O | 1.99 | 2.00 | 1.98 |

coordination of the $A'$-site Mn. The parameters observed experimentally show quite good agreement with the predicted values listed in Table 1. The discrepancies between the experimental results and the calculated ones were less than 0.9% for the lattice parameters and less than 1.7% for the bond lengths and bond angles. The results also demonstrate that the structural stability calculations based on the BVS provide a good indicator for the syntheses of novel materials.

In $A^{3+}Mn^{3+}{}_3Al^{3+}{}_4O^{2-}{}_{12}$, $Mn^{3+}$ at the $A'$ site is magnetic, whereas $Al^{3+}$ at the $B$ site is nonmagnetic. Of the three compounds prepared in the present study, $YMn_3Al_4O_{12}$ is the only one with magnetic properties due only to the $A'$-site $Mn^{3+}$ spins. The temperature dependence of the magnetic susceptibility $\chi(T)$ of $YMn_3Al_4O_{12}$ and the second-order derivative $d^2\chi(T)/dT^2$ are shown in Figure 4, and the field dependence of the magnetization of $YMn_3Al_4O_{12}$ at 5 K is shown in Figure 5. As we discussed in Ref. 8, the anomaly in $\chi(T)$ at 35 K corresponds to the antiferromagnetic transition of the high-spin $Mn^{3+}$ with $S = 2$ at the $A'$ site. The antiferromagnetic interaction should be attributed to the direct exchange interactions between the adjacent $Mn^{3+}$ ions with half-filled $d_{z^2}$ and $d_{xy}$ orbitals directed to each other. This is in sharp contrast to the ferromagnetism in $CaCu_3B_4O_{12}$ ($B$ = Ge and Sn), where ferromagnetic direct exchange interaction takes place between $Cu^{2+}$ ions with $d^9$ configuration.[9] The small inclusion of Mn ions at the $B$ site is expected to generate impurity spins in the nonmagnetic Al-sublattice, which should be responsible for the small increase of the magnetic susceptibility below 20 K.

As shown in Figure 4, magnetic transitions were not clearly seen in the magnetic susceptibility measurements for $YbMn_3Al_4O_{12}$ and $DyMn_3Al_4O_{12}$, probably because of the large contribution of the $Yb^{3+}/Dy^{3+}$ moments. The temperature dependence of $d^2\chi(T)/dT^2$, however, showed anomalies at 29 K for $YbMn_3Al_4O_{12}$ and 40 K for $DyMn_3Al_4O_{12}$ that were similar to the anomaly at 35 K for $YMn_3Al_4O_{12}$. One can expect antiferromagnetic direct exchange interaction between the $Mn^{3+}$ spins in (Yb/Dy)$Mn_3Al_4O_{12}$, considering the similarity of their crystal structure with $YMn_3Al_4O_{12}$. The anomalies at 29 and 40 K should therefore also correspond to

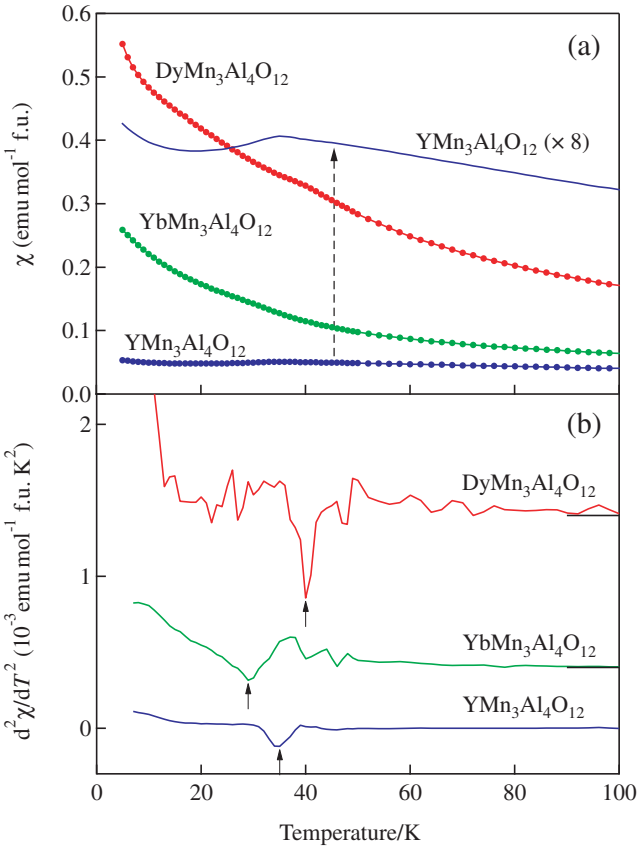


**Figure 4.** Temperature dependence of (a) the field-cooled magnetic susceptibility $\chi$ of $A$Mn$_3$Al$_4$O$_{12}$ ($A$ = Y, Yb, and Dy) measured at 2 kOe and (b) the second-order derivative $d^2\chi/dT^2$.

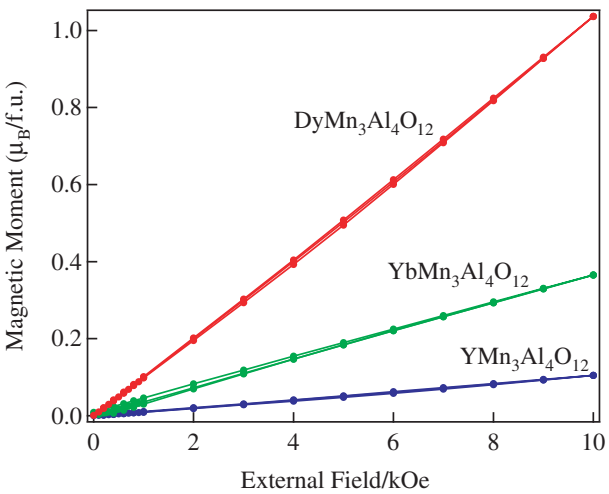


**Figure 5.** Isothermal magnetization of $A$Mn$_3$Al$_4$O$_{12}$ ($A$ = Y, Yb, and Dy) at 5 K.

the antiferromagnetic orderings of the high-spin $Mn^{3+}$ with $S = 2$ at the $A'$ site. The observed linear behaviors of the field dependence of the magnetizations at 5 K (Figure 5) are consistent with the antiferromagnetism as well. The large increase in the susceptibilities below the transition temperatures suggests paramagnetic behaviors of the $Yb^{3+}/Dy^{3+}$ moments at the $A$ site down to 5 K. The impurity spins of the Mn

inclusion in the Al-sublattice should also give paramagnetic contribution as well. Thus only the $A'$-site $Mn^{3+}$ spins appear to undergo antiferromagnetic ordering.

## Conclusion

Structural stability of hypothetical $A$-site-ordered perovskites with the formula $AMn_3Al_4O_{12}$ ($A$ = lanthanoids, Y) was evaluated by the global instability index calculated from the *SPuDS* program. Based on the results, we designed a few new $A$-site-ordered perovskites, $AMn_3Al_4O_{12}$ ($A$ = Y, Yb, or Dy), and these compounds were synthesized with a high-pressure technique. The crystal structures of the obtained compounds were characterized by synchrotron X-ray powder diffraction. In all three compounds a large $a^+a^+a^+$-type tilting of essentially rigid $AlO_6$ octahedra is stabilized by the large difference in the ionic sizes of $A^{3+}$ and $Mn^{3+}$, resulting in a fourfold square-planar coordination for $Mn^{3+}$ at the originally twelve coordinate $A$ site of the simple $ABO_3$ perovskite structure. The refined crystal structures for all three compounds were in good agreement with the values predicted by *SPuDS*. The results demonstrate that the structural stability calculations based on the bond valence sum rule provide a good indicator of what new materials can be synthesized.

The synthesized compounds contained magnetic $Mn^{3+}$ ions with $S = 2$ spins at the $A'$ site. Magnetization measurements for all three compounds revealed antiferromagnetic orderings of $Mn^{3+}$ spins. These orderings were evident at temperatures ranging from 29 to 40 K and are due to the direct exchange interaction. The $Yb^{3+}/Dy^{3+}$ moments in $(Yb/Dy)Mn_3Al_4O_{12}$ showed paramagnetic behaviors even below $T_N$ and only $Mn^{3+}$ spins contributed to the antiferromagnetic orderings.

We thank M. Azuma for fruitful discussions. This work was partly supported by the Global COE Program (No. B09), Grants-in-Aid for Scientific Research (Nos. 17105002, 19GS0207, 19014010, and 19340098), and a grant for the Joint Project of Chemical Synthesis Core Research Institutions from MEXT of Japan. P. M. Woodward acknowledges the Center for Emergent Materials at the Ohio State University, an NSF MRSEC (Award Number DMR-0820414), for supporting this research. The synchrotron X-ray diffraction experiments were performed with the approval of the Japan Synchrotron Radiation Research Institute (No. 2009B-1360).

## References

1 M. A. Subramanian, D. Li, N. Duan, B. A. Reisner, A. W. Sleight, *J. Solid State Chem.* **2000**, *151*, 323.
2 Z. Zeng, M. Greenblatt, M. A. Subramanian, M. Croft, *Phys. Rev. Lett.* **1999**, *82*, 3164.
3 J. A. Alonso, J. Sánchez-Benítez, A. De Andrés, M. J. Martínez-Lope, M. T. Casais, J. L. Martínez, *Appl. Phys. Lett.* **2003**, *83*, 2623.
4 K. Takata, I. Yamada, M. Azuma, M. Takano, Y. Shimakawa, *Phys. Rev. B* **2007**, *76*, 024429.
5 Y. W. Long, N. Hayashi, T. Saito, M. Azuma, S. Muranaka, Y. Shimakawa, *Nature* **2009**, *458*, 60.
6 B. Bochu, J. Chenavas, J. C. Joubert, M. Marezio, *J. Solid State Chem.* **1974**, *11*, 88.
7 Y. Long, T. Saito, M. Mizumaki, A. Agui, Y. Shimakawa, *J. Am. Chem. Soc.* **2009**, *131*, 16244.
8 T. Tohyama, T. Saito, M. Mizumaki, A. Agui, Y. Shimakawa, *Inorg. Chem.* **2010**, *49*, 2492.
9 Y. Shimakawa, H. Shiraki, T. Saito, *J. Phys. Soc. Jpn.* **2008**, *77*, 113702.
10 M. W. Lufaso, P. M. Woodward, *Acta Crystallogr., Sect. B* **2001**, *57*, 725.
11 M. W. Lufaso, P. W. Barnes, P. M. Woodward, *Acta Crystallogr., Sect. B* **2006**, *62*, 397.
12 S.-H. Byeon, M. W. Lufaso, J. B. Parise, P. M. Woodward, T. Hansen, *Chem. Mater.* **2003**, *15*, 3798.
13 S.-H. Byeon, S.-S. Lee, J. B. Parise, P. M. Woodward, N. H. Hur, *Chem. Mater.* **2004**, *16*, 3697.
14 S.-H. Byeon, S.-S. Lee, J. B. Parise, P. M. Woodward, N. H. Hur, *Chem. Mater.* **2005**, *17*, 3552.
15 S.-H. Byeon, S.-S. Lee, J. B. Parise, P. M. Woodward, *Chem. Mater.* **2006**, *18*, 3873.
16 A. M. Glazer, *Acta Crystallogr., Sect. B* **1972**, *28*, 3384.
17 F. Izumi, T. Ikeda, *Mater. Sci. Forum* **2000**, *321–324*, 198.